JOURNAL OF SPACECRAFT AND ROCKETS
Vol. 40, No. 5, September–October 2003
This paper reprinted from Journal of the Aerospace Sciences, Vol. 29, No. 9, 1962, pp. 1038–1051

Blunt-Nose Inviscid Airflows With Coupled Nonequilibrium Processes†

J. GORDEN HALL, ALAN Q. ESCHENROEDER, AND PAUL V. MARRONE

Cornell Aeronautical Laboratory, Inc.

Summary

Analyses have been made of the effects of coupled chemical rate processes in external inviscid hypersonic airflows at high enthalpy levels. Exact (numerical) solutions have been obtained by the inverse method for inviscid airflow over a near-spherical nose under flight conditions where substantial nonequilibrium prevails through the nose region. Typical conditions considered include nose radii of the order of 1 ft at an altitude of 250,000 ft and velocities of 15,000 and 23,000 ft per sec.

The results illustrate the general importance of the coupling among the reactions considered. These included dissociation-recombination, bimolecular-exchange, and ionization reactions. The exact solutions show the bimolecular, NO exchange reactions to be important in blunt-nose flow for the kinetics of NO and N, as they are in the case of a plane shock wave. An important difference between blunt-nose flow and plane shock flow, however, is the gasdynamic expansion in the curved shock layer of the former. This expansion reduces post-shock reaction rates. As a consequence, in the regime studied the oxygen and nitrogen-atom concentrations tend to freeze in the nose region at levels below those for infinite-rate equilibrium. The reduction below the equilibrium dissociation level can be large, particularly for nitrogen dissociation at higher velocities.

In the regime considered, the chemical kinetics are dominated by two-body collision processes. The inviscid nose flow, including coupled nonequilibrium phenomena, is thus amenable to binary scaling for a given velocity. The binary scaling is demonstrated for a range of altitude and scale by correlation of the exact solutions for given velocity and a constant product of ambient density and nose radius. This similitude, which can also scale viscous nonequilibrium and radiation phenomena in the shock layer, provides a useful flexibility for hypersonic testing where it is applicable.

The afterbody inviscid-flow problem is briefly discussed in the light of the results for the nose flow.

† Based on IAS Paper No. 62-67 presented at the 30th Annual IAS Meeting, New York, January 1962. This work was supported by the Office of Scientific Research, Mechanics Div., under Contract No. AF 49(638)-792, and is a part of Project Defender, sponsored by the Advanced Research Projects Agency, Department of Defense, and by CAL Internal Research.

* Assistant Head, Aerodynamic Research Dept.

** Research Aeronautical Engineer.

*** Research Aerodynamicist.

Received March 15, 1962. Revised and Received June 18, 1962.

The authors are pleased to acknowledge fruitful discussions with colleagues on various aspects of this paper. Comments and suggestions from Dr. W. E. Gibson and Dr. C. E. Treanor of the Aerodynamic Research Dept. were especially helpful.

The authors also wish to acknowledge the valuable assistance of L. Garr in the programing of the numerical solutions. This was done under the direction of Dr. John Fleck, without whose efforts the successful development of the machine programs would not have been possible.

Symbols

h = specific static enthalpy
J_i = net rate of reaction i per unit mixture mass
p = static pressure
q = fluid velocity
Q_{ij} = volume rate of production of species M_j from reaction i
r = radial distance coordinate
R_{Fi} = forward rate of reaction i
R_{Ri} = reverse rate of reaction i
R_0 = universal gas constant
R_S = shock wave radius at axis of symmetry
S = distance along streamline
T = translational temperature of gas
u = velocity component in x' direction
U_∞ = flight velocity
v = velocity component in y direction
x' = distance coordinate along shock wave
x = x'/R_S
y = distance coordinate normal to shock wave
z = altitude
Z = axial-distance coordinate
ρ = fluid density
δ = body-surface coordinate measured normal to shock
δ_0 = shock standoff distance at axis of symmetry
θ = angle to axis of symmetry

Subscripts

∞ = denotes free-stream or ambient flight condition

(1) Introduction

CONSIDERABLE EFFORT is now being devoted to the study of thermochemical nonequilibrium effects occurring in high-enthalpy airflows about blunt bodies and in hypersonic nozzles. Exact analyses of these effects entail simultaneous solution of the basic fluid-dynamic equations plus a set of (coupled) phenomenologic rate equations governing the nonequilibrium rate processes involved. In such analyses, two complications arise. First, a precise specification of the appropriate system of rate equations is precluded by uncertain knowledge of high-temperature air kinetics. Second, the addition of coupled nonlinear rate equations greatly increases the difficulties of analysis even when numerical methods are employed. As a consequence of these complications, many previous analyses of nonequilibrium flows have employed simplified chemical-kinetic models involving a single rate process only. Thus, for example, much work has been done for the single dissociation-recombination reaction of a diatomic gas, as this characterizes the kinetic behavior of oxygen

in air under some circumstances. For the blunt-nose problem, Freeman[1] employed the ideal dissociating gas model introduced by Lighthill, along with Newtonian flow simplifications, in a study of nonequilibrium flow about a sphere. A pure diatomic gas model was also employed by Lick,[2] who applied the inverse method in a numerical study of nonequilibrium blunt-nose flow. A survey of the literature on nonequilibrium-flow studies in this class has been given by Li.[3]

Studies entailing but a single dissociation-recombination reaction have unquestioned value in various respects. However, such a simplified picture of the kinetics of high-temperature air is quite inadequate for certain aspects of many nonequilibrium airflows of current interest. This is well demonstrated by the extensive machine calculations of Duff and Davidson,[4] Lin and Teare,[5] and Wray,[6] for the inviscid nonequilibrium flow behind strong plane shock waves in air. These calculations show, for example, that bimolecular exchange reactions involving nitric oxide play a dominant role in the kinetics of formation of N and NO behind the shock wave. The nonlinear coupling among the respective rate equations, and between the chemistry and the gasdynamics, produces a very complex situation in detail. Nevertheless, such nonlinear coupling effects are basic to the problem and must be included if realistic answers are desired.

As recently reviewed by Wray,[6] experimental shock-tube studies of high-temperature air kinetics done in the past few years have yielded considerable information on the rates of significant reactions. No doubt the knowledge of air kinetics will continue to improve. However, the present state of knowledge does appear to warrant analysis of coupled rate processes in hypersonic airflows of greater gasdynamic complexity than for the normal shock wave. In particular, nonequilibrium coupled-reaction airflows over blunt re-entry bodies and in high-enthalpy nozzles are of current interest. Work on these problems has been underway at Cornell Aeronautical Laboratory for some time as part of a broader research effort on hypersonic flows.[7–13] The recent work in this area of other groups is also noted. Vincenti[14] has reported on the development of a machine program for computing streamtube airflows involving complex coupled chemistry. Vaglio-Laurin and Bloom[15] and Lin and Teare[16] have applied streamtube methods with coupled chemistry to simplify the numerical study of nonequilibrium airflows about blunt bodies.

In the studies of inviscid nonequilibrium airflows with coupled chemistry carried out at CAL, methods were first developed for numerical solution of generalized streamtube flows as well as plane shock flow. The streamtube methods have been applied to the study of nonequilibrium airflows both in hypersonic nozzles and also over hemisphere-cylinders in re-entry flight.[9–11, 13] The streamtube approach to the latter (blunt-nose) problem has been similar to that of Refs. 15 and 16. An appropriate gasdynamic boundary condition is assumed, a priori, on the streamtube flow in order to obtain a problem with but one spatial variable. Usually the streamtube pressure distribution is assumed, some type of approximation being made on the basis of corresponding frozen or equilibrum-flow solutions, or on Newtonian or blast-wave simplifications. The detailed nonequilibrium chemistry along the streamtube is then obtained by numerical solution of a system of ordinary differential equations subject to the assumed pressure. It has been shown that the chemistry is not too sensitive to the details of the chosen pressure distribution.[15] Of course, this simplified approach cannot predict the effects of chemical nonequilibrium on the flow field pressure.

While such streamtube methods for the nonequilibrium blunt-nose problem provide valuable insight into the nonequilibrium chemistry, there remains a need for more refined approaches. Exact solutions are desirable for the nonequilibrium gasdynamics as well as the chemistry throughout the blunt-nose field. Toward this end, the inverse method as applied by Lick for a pure diatomic gas has been developed at CAL for a general chemical-kinetic model of air.[8,10] The present paper deals with application of this inverse method to the study of inviscid nonequilibrium airflow with coupled reactions over an axisymmetric, near-spherical noise.

In what follows, the coupled-reaction air model assumed is first outlined. The inviscid, nonequilibrium airflow over a blunt nose is then discussed qualitatively in terms of the corresponding nonequilibrium airflow behind a plane shock wave. Here, the concept of binary scaling for the nose flow is also outlined. Following this, specific applications of the inverse method for a near-spherical nose flow are described in detail. The emphasis here is on the results; some details of the method have been given in previous reports,[8] and a complete description is to be published. Particular attention is devoted to the importance of the coupled reactions, to the tendency for oxygen and nitrogen atom concentrations to freeze within the nose region in the flight regime studied, and to the demonstration of binary scaling by appropriate correlation of the exact nonequilibrium-flow solutions. Finally, some possible simplifications of the afterbody inviscid-flow problem suggested by the results of the nose-flow study are mentioned.

(2) Chemical Kinetic Air Model

For the thermodynamic conditions appropriate to the dissociated shock layer on a blunt nose at high altitudes, air was assumed to be an ideal-gas mixture of monatomic and diatomic constituents. The neutral species included were the atoms N, O, and Ar, and the diatomic molecules O_2, N_2 and NO. This composition neglects more complex molecules, such as the higher oxides of nitrogen, which are usually unimportant at high temperatures. In the velocity or temperature

range of interest (velocities up to 23,000 ft per sec) the dominant positive ion is NO^+. For simplicity, the nonneutral species were therefore taken to include only NO^+ and e^- in the present studies. It may be noted that the machine code developed for application of the inverse method can accommodate an arbitrary number of species and appropriate reactions. At higher velocities than considered here the nonequilibrium streamtube calculations of Eschenroeder *et al.*[13] indicate that atomic and additional molecular ions need to be included, together with additional reaction mechanisms.

The mixture of particles was assumed to remain translationally equilibrated. Rotational degrees of freedom were assumed to be equilibrated with translation. As regards vibrational excitation, this was assumed to be fully equilibrated also. This assumption, that the vibrational relaxation processes are fast compared with those for chemical change, is more serious, of course, than for rotation. However, for the main purposes of the present studies, particularly the question of binary scaling, the assumption is not critical. It is satisfied behind plane shocks in air at lower temperatures where vibrational equilibrium is attained before significant molecular dissociation occurs. At higher temperatures, the two processes are coupled. However, a well-established theoretical basis for handling such coupling in air does not presently exist. The effect of vibrational nonequilibrium on the rate of molecular dissociation in a shocked diatomic gas is accounted for in the coupled vibration-dissociation model introduced by Hammerling *et al.*[17] A more complete coupling model for a diatomic gas, which accounts also for the effect of dissociation on the rate of vibrational relaxation, has been discussed by Treanor and Marrone.[18]

In the present work, some normal shock and nose-flow studies were carried out with a postulated vibration-dissociation coupling mechanism similar to that of Ref. 17. These studies suggest that for normal-shock-type flows, at least, the overall effects of vibrational relaxation on the airflow chemistry at high temperatures are relatively limited.

Electronic relaxation was not considered. Equilibrium contributions to the internal energy were assumed for the electronic degrees of freedom.

(2.1) *Reaction System Assumed*

The chemical reactions controlling the production and removal of the neutral species were in most cases assumed as follows:

$$(1)\quad O_2 + M \underset{k_{R_1}}{\overset{k_{F_1}}{\rightleftarrows}} 2O + M$$

$$(2)\quad N_2 + M \rightleftarrows 2N + M$$

$$(3)\quad NO + M \rightleftarrows N + O + M$$

$$(4)\quad N + O_2 \rightleftarrows NO + O$$

$$(5)\quad O + N_2 \rightleftarrows NO + N$$

where the symbol M represents any atom or molecule. This reaction system has been discussed and used previously by several authors—e.g., Ref. 4—as representative of the significant kinetics of neutral species in air at the temperatures considered. Reactions (1) to (3) involve molecule dissociation by two-body collisions and atom recombination by three-body collisions. Reactions (4) and (5) are bimolecular exchange reactions involving the production and consumption of NO. From normal shock wave studies,[4–6] and from the present work, it appears as if these exchange reactions are generally important with respect to the kinetics of NO and N but play a more limited role with respect to O_2 and O. The kinetics of the latter are controlled to a large measure by the dissociation-recombination reaction (1). Reaction (2), involving the direct dissociation of N_2, appears relatively unimportant over a wide range of gasdynamic conditions, particularly at lower temperatures.

The bimolecular reaction

$$(6)\quad N_2 + O_2 \rightleftarrows 2NO$$

for production of NO was included in some of the present normal shock studies in addition to reactions (1) to (5). The results here, as previously obtained elsewhere,[6] show that at high temperatures reaction (6) is significant for NO production only at very early times—i.e., close to the shock front. The overall composition and thermodynamic effects of the reaction at high temperatures are generally rather small.

For the present temperature and pressure range the degree of ionization is relatively small. As a consequence, the ionization kinetics have little influence on the flow thermodynamics and can generally be decoupled from the problem. The only reaction mechanism considered for ionization was the dissociative recombination of NO^+—i.e.,

$$(7)\quad NO^+ + e^- \rightleftarrows N + O$$

It may be noted that at higher velocities than considered here the energy in ionization can become a significant part of the total enthalpy. In this case, the ionization kinetics cannot be decoupled from the problem. As previously noted, the nonequilibrium streamtube calculations of Ref. 13 indicate that atomic and additional molecular ions need to be considered at higher velocities, along with additional kinetic mechanisms such as charge transfer, mutual neutralization, and impact ionization processes.

(2.2) *Formulation of Rate Equations*

The formulation of the phenomenological rate equations for such a system of reactions is discussed in detail by Penner.[19] The ith of r reactions involving species M_j ($j = 1, 2 \ldots s$) is represented as

$$\sum_{j=1}^{s} \nu_{ij} M_j \underset{k_{Ri}}{\overset{k_{Fi}}{\rightleftarrows}} \sum_{j=1}^{s} \nu_{ij}' M_j \quad (i = 1, 2 \ldots r)$$

where ν_{ij} and ν_{ij}' are the stoichiometric coefficients of M_j on the left and right sides, respectively. The net

TABLE 1. Dependence of Rates of Reaction on Density, Temperature, and Mass Concentrations (T in °K.)

	REACTION	Approximate Equilibrium Constant $K_{e_i} = \frac{k_{Fi}}{k_{Ri}}$ (Ref. 6)	Forward Rate of Reaction R_{Fi}	Reverse Rate of Reaction R_{Ri}
1	$O_2 + M \underset{k_{R1}}{\overset{k_{F1}}{\rightleftarrows}} 2O + M$	$\frac{1.2 \times 10^3}{T^{1/2}} \exp(-\frac{59,000}{T})$ moles/cm^3	$\sim \frac{\rho}{T^{3/2}} \gamma_{O_2} \gamma_M \exp(-\frac{59,380}{T})$	$\sim \frac{\rho^2}{T} \gamma_O^2 \gamma_M$
2	$N_2 + M \rightleftarrows 2N + M$	$18 \exp(-\frac{112,450}{T})$ moles/cm^3	$\sim \frac{\rho}{T^{3/2}} \gamma_{N_2} \gamma_M \exp(-\frac{113,260}{T})$	$\sim \frac{\rho^2}{T} \gamma_N^2 \gamma_M$
3	$NO + M \rightleftarrows N + O + M$	$4.0 \exp(-\frac{75,000}{T})$ moles/cm^3	$\sim \frac{\rho}{T^{3/2}} \gamma_{NO} \gamma_M \exp(-\frac{75,490}{T})$	$\sim \frac{\rho^2}{T} \gamma_N \gamma_O \gamma_M$
4	$N + O_2 \rightleftarrows NO + O$	$4.2 \exp(\frac{16,010}{T})$	$\sim \rho T^{1/2} \gamma_N \gamma_{O_2} \exp(-\frac{3,120}{T})$	$\sim \rho \gamma_{NO} \gamma_O \exp(-\frac{19,130}{T})$
5	$O + N_2 \rightleftarrows NO + N$	$4.5 \exp(-\frac{37,500}{T})$	$\sim \rho \gamma_O \gamma_{N_2} \exp(-\frac{38,000}{T})$	$\sim \rho \gamma_{NO} \gamma_N$

molar-volumetric rate of production Q_{ij} of species M_j from reaction i is expressed as

$$Q_{ij} = (\nu_{ij}' - \nu_{ij}) \left\{ k_{Fi} \rho^{\nu_i} \prod_{\alpha=1}^{s} \gamma_\alpha^{\nu_{i\alpha}} - k_{Ri} \rho^{\nu_i'} \prod_{\alpha=1}^{s} \gamma_\alpha^{\nu_{i\alpha}} \right\}$$

moles/unit volume/second, where

$$\nu_i = \sum_{\alpha=1}^{s} \nu_{i\alpha}; \quad \nu_i' = \sum_{\alpha=1}^{s} \nu_{i\alpha}'$$

and γ_α is the mass concentration of M_α in moles/unit mass. The factors k_{Fi} and k_{Ri} are the forward and reverse specific rate coefficients, respectively, of the ith reaction. These rate coefficients are assumed to depend only on the translational temperature T for vibrational equilibrium. A net rate of reaction i per unit mass of mixture, J_i, is defined as

$$J_i = Q_{ij}/[(\nu_{ij} - \nu_{ij}')\rho] = R_{F_i} - R_{R_i}$$

moles/gm sec, where R_{Fi} and R_{Ri} are the corresponding forward and reverse rates of reaction. Thus J_i gives the net molar rate of production in the forward direction of reaction i per unit mass of mixture for unit stoichiometric change. Table 1 shows the dependence of R_{Fi} and R_{Ri} on density, temperature, and species mass concentrations for reactions (1) to (5).

For equilibrium $Q_{ij} = 0$, and the forward and reverse rate coefficients for any reaction are related through a corresponding equilibrium constant $K_{ei} = k_{Fi}/k_{Ri}$. The equilibrium constants are known functions of the translational temperature determined from statistical mechanical calculations. With vibrational equilibrium assumed, the relation $k_{Fi}/k_{Ri} = K_{ei}(T)$ is usually applied also for $Q_{ij} \neq 0$. This was done in the present work.

With transport-free flow, as assumed, the total time rate of change of γ_j becomes

$$\frac{D}{Dt} \gamma_j = \frac{1}{\rho} \sum_{i=1}^{r} Q_{ij}$$

The system of rate equations so obtained must be solved simultaneously with the equations expressing thermodynamic state and conservation of energy, mass, and momentum. Thermodynamic state is expressed by

$$p = \rho R_0 T \sum_{j=1}^{s} \gamma_j$$

and energy conservation becomes

$$q^2/2 + h = \text{constant} = h_0$$

for adiabatic steady flow, as considered. The static enthalpy $h = e + (p/\rho)$ is a known function of all γ_j, T, and the molecular vibrational energies. For vibrational equilibrium, the latter are known explicitly in terms of γ_j and T. Relations for conservation of fluid mass and momentum do not involve chemical variables explicitly and therefore take the usual fluid-dynamic forms.

(2.3) *Rate Data Employed*

A tabulation of all reaction rate data employed in the present studies is given in Table 2 along with the data source. Shown here are values of the forward rate

coefficients, k_{Fi}, for the reactions as written. Reaction numbers correspond to those in the text. The flow calculations were carried out in terms of k_{Fi} and the corresponding equilibrium constant $K_{ei}(T) = k_{Fi}/k_{Ri}$. Table 1 lists convenient (approximate) analytic expressions from Ref. 6 for the equilibrium constants of reactions (1) to (5).

A comparison was made of the rate data used in the present studies, as given in Table 2, with composite values proposed in the review of Ref. 6. In general, the agreement is quite good for the important reactions. What differences do exist would not appear to be too important for the present purpose. Normal shock solutions obtained in the present studies agree reasonably well with those of Ref. 6. Of course, considerable uncertainties exist in the experimental rate data in some cases. A systematic investigation of the sensitivity of the present results to the reaction system and rate data employed was outside the scope of the work. However, some limited study in this direction was made, and some previous studies are also relevant. This question is further discussed in Section (3) in connection with specific results.

(3) Nonequilibrium Airflow Over Near-Spherical Nose

(3.1) *General Description of Flow Field*

A dominant feature of the hypersonic flow over a spherical-type nose is the strong curved shock wave which stands off from the surface a distance generally small compared with the nose radius. Immediately on crossing the curved bow shock a fluid particle begins to equilibrate its chemistry with the local thermodynamic environment. Initially, at least, the equilibration process therefore resembles that occurring behind a plane normal shock wave at the appropriate velocity and density. Thus it is anticipated that features of the nonequilibrium chemistry calculated for plane normal shocks in air[4–6] will appear along streamlines in the blunt-nose flow field. Beyond this qualitative consideration, Gibson[20, 21] has recently developed a quantitative method of using plane air-shock solutions to determine the complete blunt-nose inviscid field in the vicinity of the stagnation streamline.

Basic features of plane shock solutions for the coupled-reaction air model of Section (2) include the important effects of the bimolecular exchange reactions (4) and (5) in addition to the characteristic dissociation relaxation of oxygen and nitrogen. As previously noted, the exchange reactions play an important role with respect to the formation of NO and N. In particular, in the temperature range considered, reaction (5) (forward) dominates the production of NO and N in the initial flow behind the shock. Generally, the exchange reactions tend to a local equilibrium much faster than the dissociation-recombination reactions (1) to (3). As a consequence of this behavior, the NO concentration builds up rapidly behind the shock and overshoots its final equilibrium value attained when the entire reaction system is equilibrated. The resulting

TABLE 2. Reactions and Rate Coefficients Employed in Calculations

	REACTION	CATALYTIC BODY M	FORWARD RATE CONSTANT k_F T IN °K	UNITS OF k_F	SOURCE
1	$O_2 + M \underset{k_{RI}}{\overset{k_{FI}}{\rightleftharpoons}} 2O + M$	O_2	$3.6 \times 10^{21} T^{-3/2} \exp(-\frac{59380}{T})$	$CM^3MOLE^{-1}SEC^{-1}$	CALCULATED FROM REF. 30 DATA
		O	$2.1 \times 10^{18} T^{-1/2} \exp(-\frac{59380}{T})$	"	$35\frac{T}{\theta D}$ x RATE FOR O_2 (30)
		N_2,N,NO	$1.2 \times 10^{21} T^{-3/2} \exp(-\frac{59380}{T})$	"	$\frac{1}{3}$ x RATE FOR O_2 (31)
2	$N_2 + M \rightleftharpoons 2N + M$	N_2	$3.0 \times 10^{21} T^{-3/2} \exp(-\frac{113260}{T})$	"	VIA k_R FROM REF. 17, 31
		N	$1.5 \times 10^{22} T^{-3/2} \exp(-\frac{113260}{T})$	"	5 x RATE FOR N_2 (31)
		O_2,O,NO	$9.9 \times 10^{20} T^{-3/2} \exp(-\frac{113260}{T})$	"	$\frac{1}{3}$ x RATE FOR N_2 (31)
3	$NO + M \rightleftharpoons N + O + M$	N_2,O_2,O, N,NO,Ar	$5.2 \times 10^{21} T^{-3/2} \exp(-\frac{75490}{T})$	"	VIA k_R FROM REF. 31
4	$O_2 + N \rightleftharpoons NO + O$		$1.0 \times 10^{12} T^{1/2} \exp(-\frac{3120}{T})$	"	REF. 31
5	$N_2 + O \rightleftharpoons NO + N$		$5.0 \times 10^{13} \exp(-\frac{38000}{T})$	"	REF. 32
6	$N_2 + O_2 \rightleftharpoons 2NO$		$9.1 \times 10^{24} T^{-5/2} \exp(-\frac{65000}{T})$	"	REF. 6
7	$NO^+ + e^- \rightleftharpoons N + O$		$1.8 \times 10^{21} T^{-3/2}$	"	REF. 11, 25, 33

maximum in NO concentration is a characteristic feature over a wide range of conditions.

In the blunt-nose flow field, this picture of the nonequilibrium chemistry provided by plane shock flow is modified, of course, by the particular gasdynamic environment of the curved shock layer. On flowing around the blunt nose the velocity of a fluid particle increases while its density and temperature decrease due to gasdynamic expansion. The reduction of density and temperature generally reduces the rates of chemical reaction and slows the strong initial drive toward post-shock equilibration. Streamlines closest to the body are characterized by a strong gasdynamic expansion downstream of the sonic line which can effectively quench the chemistry and produce frozen composition in the afterbody flow.

Fluid particles crossing the curved bow shock close to the axis of symmetry where it is nearly normal encounter the most favorable conditions for attaining thermochemical equilibrium prior to leaving the immediate nose region. Here the temperature immediately behind the translational-rotational shock front is higher and the velocity lower than at any other corresponding post-shock position. For strong shock conditions the density immediately behind the shock changes little with shock angle β, and the corresponding post-shock temperature therefore varies approximately as the pressure, or as $\sin^2 \beta$. Thus, particles crossing the bow shock further from the axis encounter reduced initial temperatures and increased velocities. Both effects reduce the degree of equilibration attained over a given path length. A progressive departure from post-shock equilibration might therefore be expected on moving away from the axis along loci of equal streamline lengths. Sufficiently far from the axis the internal degrees of freedom of fluid particles crossing the curved shock may be expected to remain completely frozen at ambient conditions during particle transit over the body. However, the equilibrium excitation at the lower temperatures thus involved may be relatively unimportant.

From the foregoing consideration, it is evident that the entire nose-region inviscid flow may be expected to exhibit substantial nonequilibrium if such prevails along streamlines which cross the bow shock close to the axis. This situation was the primary concern in the present studies for flight conditions giving inviscid flow through an appreciable (outer) portion of the shock layer. A point of particular interest was the degree to which the three-body recombination reactions (1) to (3) come into play on inner streamlines before the strong gasdynamic expansion downstream of the sonic line effectively quenches the chemistry. On this point hinges the possibility of a simple density scaling of the nonequilibrium chemistry through the nose region.

(3.2) *Binary Scaling of Nonequilibrium Flow*

In chemical equilibration behind a plane shock wave in air (see, for example, the normal shock solutions of Ref. 4), the net direction of reactions (1) to (3) is dissociation. The reverse (recombination) reaction rates become equal to the forward (dissociation) reaction rates only at final equilibration. Where all three-body recombination reactions remain unimportant the nonequilibrium chemistry is determined by two-body collision processes only, since all reactions other than three-body recombination are of this class. All reaction rates J_i, therefore, have the same direct dependence on density in this case (Table 2). Thus, for given initial temperature and species mass concentrations behind the shock, the time or distance variation of all variables behind the shock may be normalized or scaled with respect to the initial (post-shock) density. For sufficiently strong shocks, the pre-shock density also normalizes the solution since the (ideal-gas) density ratio across the shock becomes essentially invariant. The same binary scaling applies with vibrational nonequilibrium if the usual two-body collisional excitation of vibration is assumed. It is required only that the effective vibrational relaxation times of the diatomic species have the usual inverse first-power dependence on the total density.

The above type of scaling is demonstrated in Ref. 4 for the features of the NO concentration maximum which accompanies reversal of reactions (4) and (5) behind strong shocks in air. At high temperatures and lower densities this NO maximum occurs when reactions (1) to (3) are still far out of equilibrium—i.e., $(R_{Fi}/R_{Ri}) \gg 1$. Under these conditions its magnitude and location are accurately scaled as above. At higher densities the recombination reactions, whose rates vary as ρ^2 (Table 2), become important at the location of the NO maximum and the scaling breaks down.[4]

Carried over to the flight situation, this binary scaling with density means that the inviscid nonequilibrium airflow over a blunt nose of given shape is scaled for a fixed (high) flight velocity U_∞ by the condition $\rho_\infty L =$ constant when three-body recombination remains unimportant. Here ρ_∞ is ambient atmospheric density and L a characteristic dimension of the flow field or body. Considering a bow shock of given shape, the fixed and high flight velocity ensures duplication of the (ideal-gas) temperature boundary conditions immediately behind the normalized shock. The relatively small variation in atmospheric temperature with altitude at conditions of interest is thus unimportant. The high velocity (Mach number) also provides the required strong-shock condition that the (ideal-gas) density ratio across the shock have its limiting value.

Conditions for which recombination is unimportant in air can be roughly estimated in terms of fluid particles crossing the bow shock close to the axis, say at a radius of order standoff distance δ_0 (Fig. 1), and the corresponding plane shock flow for air. In the case of a spherical nose, such particles experience an environment similar to that behind the corresponding plane uniform shock (at the flight velocity and density) over a path length somewhat less than the nose radius before experiencing rapid expansion downstream of the sonic region.

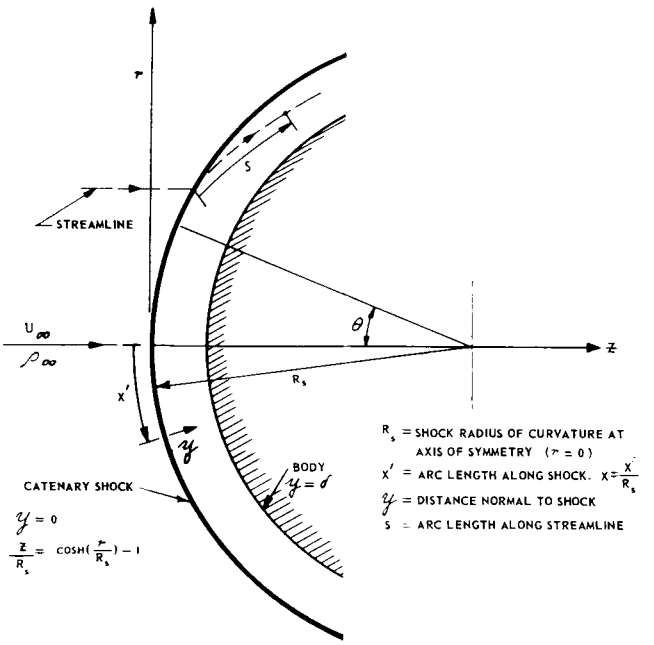

FIG. 1. Coordinate system for axisymmetric blunt-nose flows.

Therefore, if the appropriate relaxation length for the corresponding plane shock case is of the order of the nose radius or larger, recombination will be generally unimportant throughout the blunt-nose field. Here the relaxation length is the distance required for the ratios of the forward-to-reverse rates of reactions (1) to (3) to become of order 1 in the corresponding plane shock case. A characteristic feature of the plane shock in air at high temperatures and low densities is that the forward-to-reverse rate ratios of reactions (1) to (3) are approximately equal over most of the distance required for equilibration. This behavior is demonstrated by the normal shock solutions of Ref. 4, for example, in which the above relaxation length is clearly evident.

At the velocities and high-altitude densities of present interest (15,000 to 23,000 ft per sec and 150,000 to 250,000 ft altitude) the above relaxation length is typically several orders of magnitude greater than the distance to the maximum in the NO concentration previously mentioned. At the location of the latter, the forward-to-reverse rate ratios for reactions (4) and (5) are of order 1, whereas those for reactions (1) to (3) are typically several orders of magnitude.[4] Thus, another indication that recombination is unimportant through the nose region is if the distance to the NO maximum behind the corresponding plane shock approaches the order of magnitude of the shock stand-off distance, δ_0.

An important question is that of the range of validity of such scaling with respect to the parameters U_∞, ρ_∞, and $\rho_\infty L$. For increasing velocity, density, and scale, equilibration is eventually attained very rapidly behind the bow shock and recombination becomes important throughout the inner nose-region flow. Equilibrium conditions must always prevail sufficiently close to the inviscid stagnation point where the local velocity tends to zero. The practical question, then, is the region of influence of the equilibrium stagnation zone. In the real situation, viscous effects are present close to the body and need to be considered in this respect. A determination of the general limits of binary scaling was outside the scope of the present work. However, an analytic study of this question has recently been carried out by Gibson.[12, 20] The results from this study suggest a rather wide range of validity for the neglect of three-body recombination both for the Lighthill gas model and for air with coupled reactions. In particular, molecular dissociation behind the bow shock can attain a level very close to equilibrium along the stagnation streamline before atom recombination becomes important.

It may be noted that the condition $\rho_\infty L$ = constant at given velocity also has implications for the scaling of nonequilibrium radiation phenomena, as well as for nonequilibrium viscous phenomena. For nonequilibrium radiation, discussed by Camm *et al.*,[22] the correct scaling of the nonequilibrium temperature and concentration fields by this condition when recombination is unimportant means that the associated radiative heat transfer will be simultaneously scaled (reproduced) correctly if electronic equilibrium prevails. Correct scaling of radiative heat transfer with electronic nonequilibrium requires the latter to be governed by two-body collision processes. In the simultaneous scaling of nonequilibrium viscous phenomena, discussed by Gibson,[12] the preservation of Reynolds number by the above condition means that nonequilibrium viscous or boundary-layer phenomena are correctly scaled provided recombination remains unimportant in the viscous flow and appropriate surface boundary conditions are maintained. In the regime considered here, where nonequilibrium inviscid flow prevails through the outer part of the shock layer, the low-density, small-scale conditions favor occurrence of a chemically frozen boundary layer wherein atoms would diffuse to a cold surface before recombining in the gas phase.

It is apparent that such scaling offers a useful flexibility for hypersonic testing where applicable to the simulation of nonequilibrium phenomena occurring in high-altitude flight of a blunt nose. As discussed in Ref. 23, wind-tunnel duplication of the ambient conditions appropriate to re-entry flight requires nozzle reservoir pressures which become forbiddingly high for expansions to high velocities. Binary scaling could conceivably be employed to compensate for tunnel ambient pressures less than in flight by the use of a model size larger than full scale. If the flight velocity was duplicated, correct simulation of flight nonequilibrium phenomena in the nose region would thereby be attained. Although correct simulation requires duplication of the flight velocity, duplication of the flight Mach number is not essential to the nose-flow scaling provided the test Mach number is sufficiently high to ensure strong-shock conditions. Another possible application of such nonequilibrium scaling to hypersonic testing might be in ballistic range studies.

Here the use of pressures higher than in flight could compensate for small model scale.

(3.3) *Numerical Studies*

The inviscid flow field about a blunt-nosed body in supersonic flight is rendered difficult for analysis because of its mixed aerodynamic nature behind the detached shock in the nose region. In recent years, considerable emphasis has been placed on development of numerical methods, particularly for use with high-speed digital computers, for solving the subsonic-transonic field around a blunt nose under ideal-gas conditions. Both direct and inverse approaches to the problem have been developed, with the main emphasis on the hypersonic regime. In the direct approach, the flow field is determined for a specified body shape. In the inverse method, the shock-wave shape is specified and the corresponding body shape is determined by mass conservation requirements in the course of solution. While the direct method has a greater practical utility for studies of the influence of body geometry, the inverse method greatly simplifies handling of the boundary conditions at the shock wave, the location of which is unknown in the direct approach. A critical discussion of both approaches is given by Hayes and Probstein.[24]

In the present work, the development of the inverse method for a general chemical-kinetic model of air generally followed the previous work of Lick[2] for a pure diatomic gas. The method entails a numerical marching in from the starting conditions behind the specified shock wave with the fluid-dynamic and chemical rate equations of Section (2) being solved simultaneously. The starting problem is simplified by the initial nonequilibrium state whereby initial singularities are avoided in the rate equations. The computation is carried out in terms of coordinates x' and y along and normal to the shock front, respectively, as illustrated in Fig. 1. A Runge-Kutta integration procedure is used along the normal coordinate y, derivatives along x' being fitted by a seven-point formula. Specific streamline shapes may be determined from mass-flow integrals computed in the course of initial solution. The thermodynamic properties of the chemical species may be computed in either of two ways: (1) the use of polynomial fits of enthalpy with temperature as in Ref. 4, with derived relations for other quantities as free energy and entropy, and (2) the use of simple harmonic oscillator formulas where vibrational equilibrium is assumed, including lower excited levels. Simple oscillator formulas were employed for the diatomic species in the present studies.

The inverse method formulated for inviscid axisymmetric flows has been coded for high-speed digital machine computation by means of an IBM-704 computer. This code has been applied to the computation of several examples which demonstrate the previous considerations of nonequilibrium blunt-nose flow with coupled reactions. The examples were calculated for velocities of 15,000 and 23,000 ft per sec, using the chemical kinetic air model of Section (2)—i.e. reactions (1) to (5) and reaction (7), with rate data as given in Table 1. The axisymmetric shock-wave shape employed was the catenary $Z/R_s = \cosh(r/R_s) - 1$, where R_s is the shock radius of curvature at the axis. The notation is illustrated in Fig. 1.

The values of ambient density (altitude) and shock radius chosen for the calculations were selected to produce substantial departure from equilibrium throughout the nose region. In particular, for the corresponding plane normal shock solutions the NO maximum occurs at a distance behind the shock approaching the shock standoff distance δ_0. As previously noted, a determination of the limits of binary scaling was outside the scope of the work. However, in order to demonstrate scaling the values of ρ_∞ and R_s were varied for several cases so as to keep the product $\rho_\infty R_s$ constant at given velocity. A summary of conditions for the cases computed is given in Table 3. The ambient atmospheric conditions employed were those for the 1956 ARDC model atmosphere.

In general, the results for neutral species in the present blunt-nose computations would not appear to be unduly sensitive to the rate data employed. The sensitivity question here is essentially that which arises for nonequilibrium airflow behind plane uniform shocks. In the latter case, quantitative studies have been made by previous authors.[4, 25] In particular, the discussion and results herein pertaining to nonequilibrium scaling of the neutral species concentrations and the gas-dynamic field are probably unaffected by present uncertainties in the rate data. However, the same may not necessarily be true for the ionized species, as even the basic kinetic mechanisms in this case appear much less certain.

With respect to viscous effects which are present at the above conditions, the stagnation-point boundary-

TABLE 3.

Flight Velocity, U_∞, ft per sec	Altitude, z, ft $\times 10^3$	Ambient Density, ρ_∞, lb (mass)/ft^3	Shock Radius, R_s, ft
15,000	150	0.1147×10^{-3}	0.183
15,000	200	0.1950×10^{-4}	1.07
15,000	250	0.2573×10^{-5}	8.15
23,000	200	0.1950×10^{-4}	0.0692
23,000	250*	0.2573×10^{-5}	0.525

* Results for this case are from computations performed for the Air Research and Development Command, Rome Air Development Center, Griffiss Air Force Base, N. Y., under Contract No. AF 30(602)-2267.

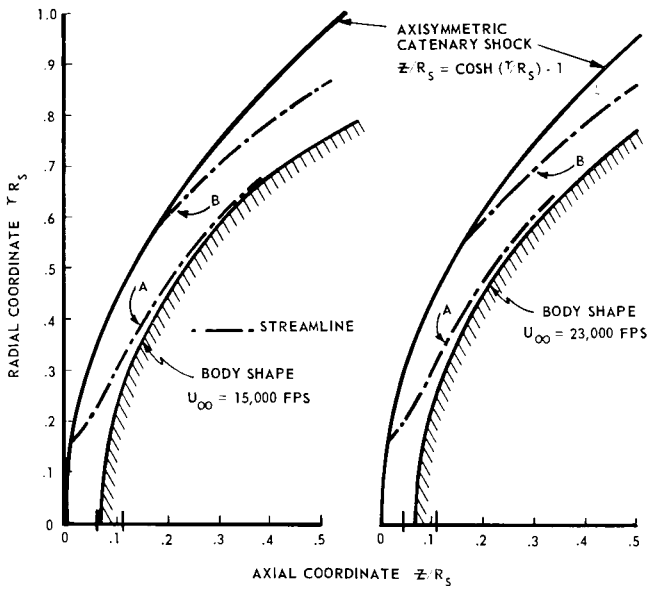

FIG. 2. Correlated body shapes and streamlines for nonequilibrium blunt-nose airflows.

layer thickness is about one fifth the shock standoff distance for the 15,000-ft-per-sec-velocity cases. For the two cases at 23,000-ft-per-sec velocity the boundary layer is relatively thicker, becoming about one half the standoff distance. These values of boundary-layer thickness are indicated by Scala[26] for typical cold-wall conditions. It will be noted that the ratio of boundary-layer thickness to nose (shock) radius R_s should remain approximately unchanged for given velocity in these examples since $\rho_\infty R_s$ remains constant. Although the presence of the boundary layer would modify the present inviscid-flow solutions for the flow close to any real body, as discussed qualitatively below, it should be emphasized that this fact does not enter, per se, the present considerations on the scaling of inviscid nonequilibrium phenomena. Also, of course, the usefulness of the present numerical results for the testing of approximate inviscid-flow solutions is unaffected by viscous phenomena.

Detailed consideration of viscous effects is outside the scope of this paper. However, it may be mentioned that the blunt-nose flow chemistry will be influenced close to a cold surface by the reduction of temperature and increase of density through the boundary layer. The net effect on reaction rates (Table 2) will tend to be a reduction where activation energies are large, as with dissociation, and an increase where density dependence dominates, as with three-body recombination. Close to a cold surface the cumulative effect of temperature reduction may therefore be expected to result in atom concentrations less than those for inviscid adiabatic flow. The associated density increase, and also the temperature decrease, will enhance recombination. However, as previously noted, the general conditions considered here favor a chemically frozen boundary layer where gas-phase recombination is unimportant.

(3.4) *Numerical Results*

The results of the numerical studies are of interest with respect to both the basic chemical and gasdynamic effects of nonequilibrium, as well as the question of binary scaling. The inverse method provides a detailed solution through the entire nose region on a mesh scale small compared with the standoff distance. The wealth of numerical data so obtained in the present examples poses a problem with respect to graphical presentation. In order to illustrate the above points of interest, detailed results are presented in Figs. 2 to 13 for distributions of gasdynamic and chemical variables along two representative streamlines, and along two rays normal to the bow shock.

The computed body shapes for the two velocities and the two streamlines, A and B, determined in each case are shown in Fig. 2. Streamline A crosses the shock inside the sonic point at an angle θ of about 9°, whereas B crosses outside the sonic point at a value of θ of about 35°. The flow patterns of Fig. 2 and the results in Figs. 3 to 12 apply to all ambient densities and scale considered for the respective velocities as the correlation or binary scaling of the different solutions for $\rho_\infty R_s$ = constant was generally excellent. This will be further considered following discussion of the variation of quantities along the two streamlines shown. It will be noted in Fig. 2 that the flow patterns for the two velocities are quite closely the same. This is coincidental and happens because the reduced scale of the higher velocity case offsets the more rapid equilibration produced by the associated higher temperature.

Distributions of pressure, density, temperature, and species mass concentrations along streamlines A and B are plotted in Figs. 3 to 8 for the two velocities. Thermogasdynamic variations along these streamlines shown in Figs. 3 and 4 are similar for the two velocities. However, it will be noted that the temperature level is roughly doubled at the higher velocity. The early flow along inner streamline A resembles that behind a plane uniform shock—i.e., increasing density and sharply decreasing temperature. Fairly quickly, however, the gasdynamic expansion becomes evident, in contrast to the plane shock flow. Thus the density and

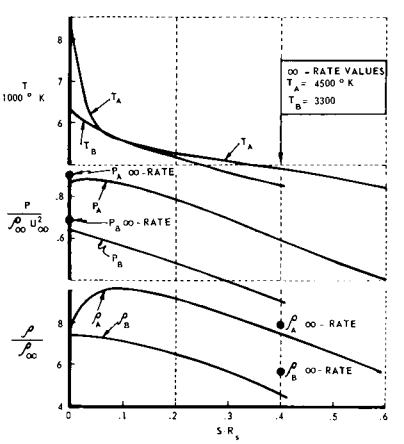

FIG. 3. Correlations of temperature (T), pressure (P) and density (ρ) along nonequilibrium blunt-nose streamlines A and B. U_∞ = 15,000 ft per sec.

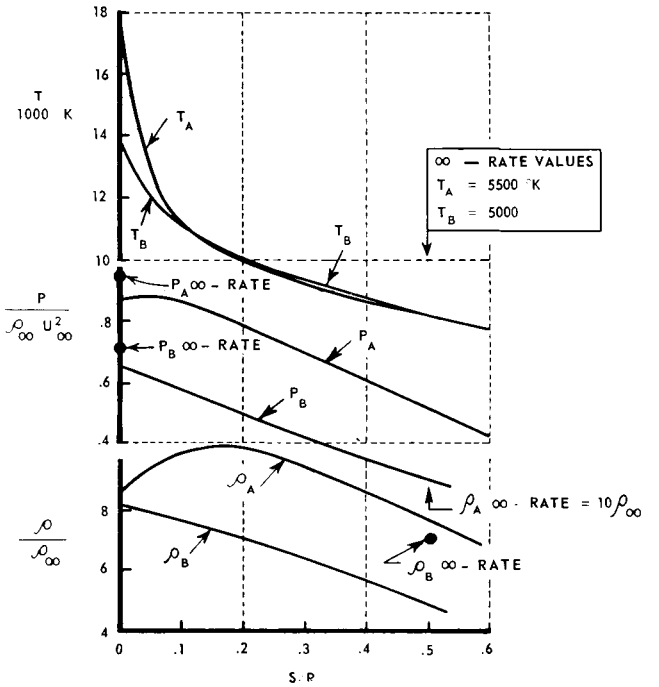

FIG. 4. Correlations of temperature (T), pressure (P) and density (ρ) along nonequilibrium blunt-nose streamlines A and B. U_∞ = 15,000 ft per sec.

pressure pass through maximums and then decrease, with corresponding decrease in temperature. The latter changes are monotonic along outer streamline B which crosses the shock outside the sonic point.

Also shown in Figs. 3 and 4 for S/R_s values of about 0.5 (S = distance along streamline) are the corresponding values of temperature and density for infinite-rate equilibrium flow. These values (and corresponding species concentrations) were computed assuming the local pressure to be unaffected by nonequilibrium. For the present purpose this assumption is quite adequate, as the effects of nonequilibrium on the pressure in this flow region are small. This is demonstrated in Figs. 3 and 4 by the infinite-rate values for pressure shown to exist immediately behind the shock (S/R_s = 0). Further evidence on this point is the close agreement between the pressure distributions of Figs. 3 and 4 where the nonequilibrium dissociation levels are high and quite different. It will be noted that the nonequilibrium temperatures substantially exceed the infinite-rate values. This is primarily because of the lag in oxygen dissociation at 15,000 ft per sec (Fig. 3) and the lag in nitrogen dissociation at 23,000 ft per sec (Fig. 4).

The corresponding distributions along streamlines A and B of the chemical species O, N, NO, and e^- are shown in Figs. 5 to 8, respectively. In these figures, the species concentrations are plotted on a mass basis as moles/original mole of air so that they become constant for constant or frozen composition.

Figs. 5 and 6 show that oxygen dissociation is thermodynamically important at both velocities. Nitrogen dissociation is unimportant in this sense at the lower velocity of 15,000 ft per sec, but is very significant at 23,000 ft per sec. The oxygen atom concentrations level off somewhat below the infinite-rate values on both streamlines at 23,000 ft per sec and on inner streamline A at 15,000 ft per sec. It will be noted that the infinite-rate values here represent essentially complete O_2 dissociation. Along outer streamline B at 15,000 ft per sec, O freezes well below equilibrium. In all cases, nitrogen atom concentrations remain well below the infinite-rate values. Thus, at 23,000-ft-per-sec velocity, the energy in the dissociation of nitrogen, although large, is only of the order of one half or less of the infinite-rate equilibrium value.

The NO concentrations of Figs. 7 and 8 show expected maximums on inner streamline A, but remain well above infinite-rate values. Maximums are not attained on outer streamline B, and at 15,000 ft per sec the infinite-rate value here is not exceeded. On outer streamlines such as B, where the temperature level is progressively reduced and the O_2 and N_2 concentrations become relatively high, reaction (6) could appreciably accelerate the formation of NO. Similar maximums are observed in the e^- concentration along inner streamline A. The electron concentrations tend to remain above infinite-rate values.

The results of Figs. 3 to 8 illustrate points of the previous discussion of Section (3.1) on the qualitative features to be expected in the nonequilibrium blunt-nose flow field. In particular, a progressive departure from equilibrium occurs on moving towards outer streamlines in the field (A to B) along loci of equal streamline lengths (equal S/R_s values). Features of plane normal shock flows with coupled reactions appear along individual streamlines, such as the maximum in NO concentration. The relative importance of individual reactions along streamlines is qualitatively as for plane shock flows at the appropriate temperature level. Thus, reaction (1) dominates O_2 dissociation, whereas reaction (2) for N_2 dissociation tends to be relatively unimportant. Reactions (3), (4), and (5) are important for the kinetics of N and NO. A basic difference from plane shock flow is the continued reduction in temperature and density with flow expansion around the nose. This reduces the rates of all reactions and, as

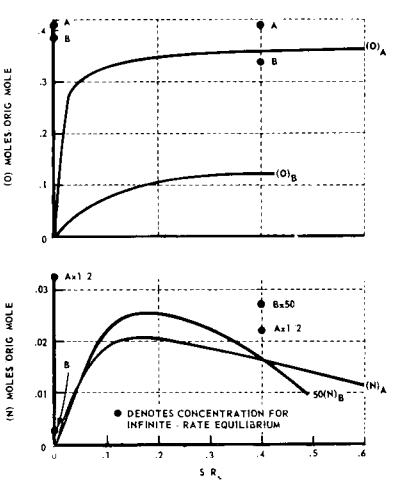

FIG. 5. Correlations of oxygen (O) and nitrogen (N) atom concentrations along nonequilibrium blunt-nose streamlines A and B. U_∞ = 15,000 ft per sec.

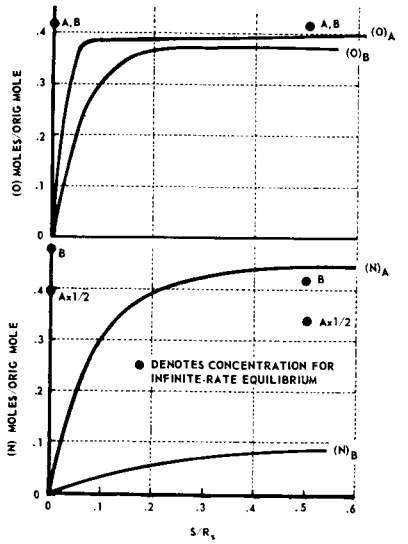

FIG. 6. Correlations of oxygen (O) and nitrogen (N) atom concentrations along nonequilibrium blunt-nose streamlines A and B. U_∞ = 23,000 ft per sec.

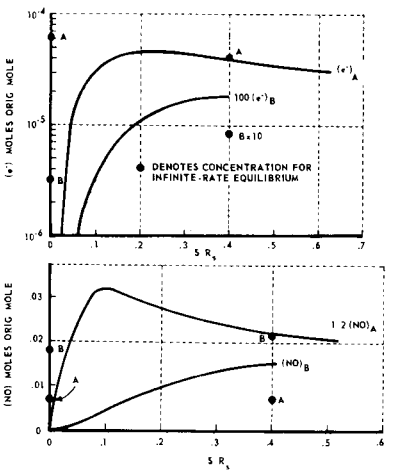

FIG. 7. Correlations of nitric oxide (NO) and electron (e^-) concentrations along nonequilibrium blunt-nose streamlines A and B. U_∞ = 15,000 ft per sec.

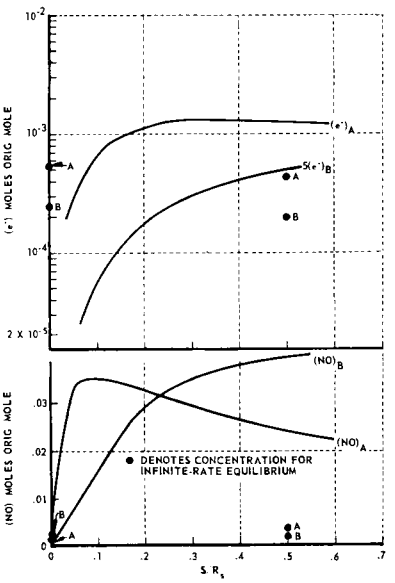

FIG. 8. Correlations of nitric oxide (NO) and electron (e^-) concentrations along nonequilibrium blunt-nose streamlines A and B. U_∞ = 23,000 ft per sec.

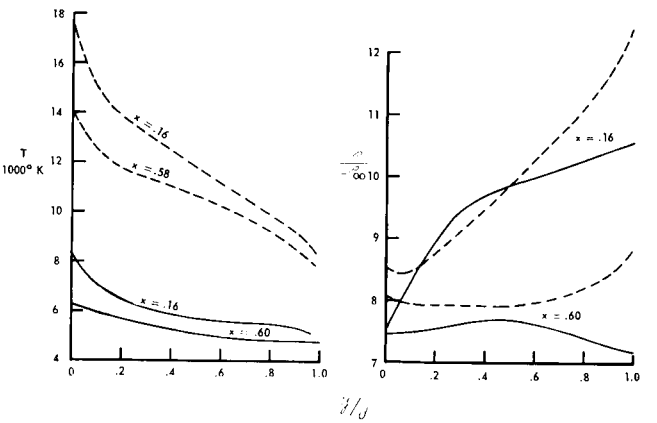

----- = 23,000 ft per sec
——— = 15,000 ft per sec

FIG. 9. Correlations of temperature (T) and density (ρ) across nonequilibrium blunt-nose shock layer.

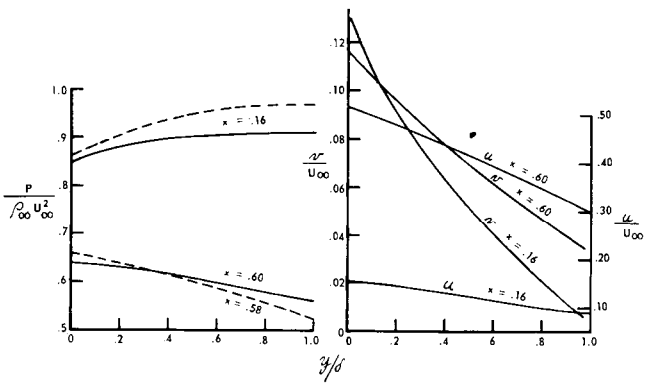

----- = 23,000 ft per sec
——— = 15,000 ft per sec

FIG. 10. Correlations of pressure (P) and velocity components normal (v) and parallel (u) to shock across nonequilibrium blunt-nose shock layer.

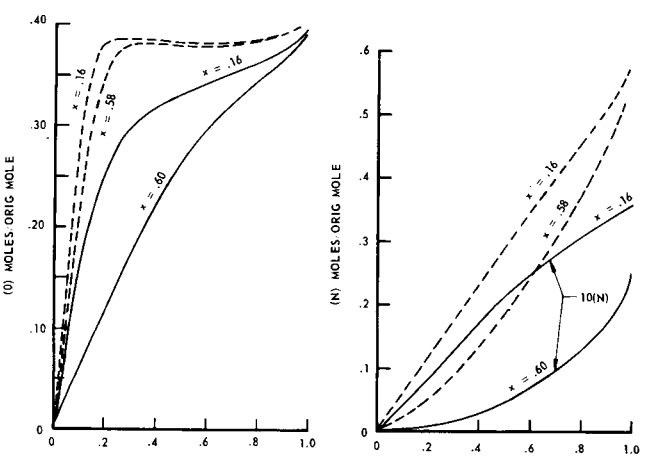

----- = 23,000 ft per sec
——— = 15,000 ft per sec

FIG. 11. Correlations of oxygen (O) and nitrogen (N) atom concentrations across nonequilibrium blunt-nose shock layer.

illustrated by the solutions, enhances the lag in dissociation in such a way that atom concentrations tend to freeze.

Figs. 9 to 12 show distributions of thermodynamic and chemical variables across the shock layer along two rays normal to the shock at values of x equal to 0.16 ($\theta \simeq 9°$) and 0.58 or 0.60 ($\theta \simeq 35°$). These distributions reflect the different particle histories experienced along the respective streamlines intercepted. In general, the gas state approaches equilibrium on moving along a ray toward the body. Of the gasdynamic features of these results, it will be noted in Fig. 10 that the normalized pressure distributions across the shock layer are relatively insensitive to the very significant changes in the nonequilibrium chemistry (particularly in atom concentrations) which occur in going from a velocity of 15,000 ft per sec to one of 23,000 ft per sec. A similar insensitivity of the normalized pressure to the chemistry was noted for the streamline pressure distributions of Figs. 3 and 4. Also in Fig. 10 it will be seen that the velocity distributions across the shock layer tend to remain nearly linear as in the case of ideal-gas flow.[27] Features of the chemistry which may be noted in Figs. 11 and 12 are the greatly increased concentrations of O, N, and e^- and the decreased concentration of NO which obtain generally throughout the nose region at the higher velocity of 23,000 ft per sec. Although the body scales are quite different for the two velocities, these effects are due primarily to the higher temperatures existing at 23,000 ft per sec.

Values of the shock standoff distance at the axis, δ_0, are given in Table 4. Corresponding values for infinite-rate equilibrium, completely frozen chemistry, and ideal-gas flow determined by the method of Li and Geiger[28] are shown for comparison. It is of interest to note that the values of δ_0 for the present nonequilibrium flows tend to lie closer to the equilibrium than to the chemically-frozen or ideal-gas values. By virtue of the binary scaling discussed below, the above values of δ_0 for nonequilibrium flow also apply to the additional cases computed for 150,000 and 250,000-ft altitude at 15,000 ft per sec and for 250,000-ft altitude at 23,000 ft per sec. The values of δ_0 for these additional cases agree with the above values to within the numerical accuracy of the determination of δ_0 — namely, to within about 1 percent or better.

With respect to the question of binary scaling, the results for the cases computed for different altitudes at given velocity with $\rho_\infty R_s$ held constant show excellent agreement. The results of Figs. 2 to 12 thus apply for all cases computed at the respective velocities to an accuracy generally of the order of 1 percent or better. The excellent correlation obtained in this respect implies that three-body recombination is generally unimportant for the conditions considered. This is demonstrated directly in Fig. 13, which shows the ratios of the forward-to-reverse reaction rates (R_{F_i}/R_{R_i}) of all reactions along streamline A for both velocities at an altitude of 200,000 ft. The unimportance of three-body recombination through reactions (1), (2), and (3) is apparent here. This is particularly true for the smaller-scale, higher-velocity case at 23,000 ft per sec because of the much smaller particle flow time at a given value of S/R_s than at 15,000 ft per sec. For the different altitude cases, the curves in Fig. 13 for reactions (1), (2), and (3) shift inversely as the change in ambient density, whereas those for reactions (4), (5), and (7) remain unchanged.

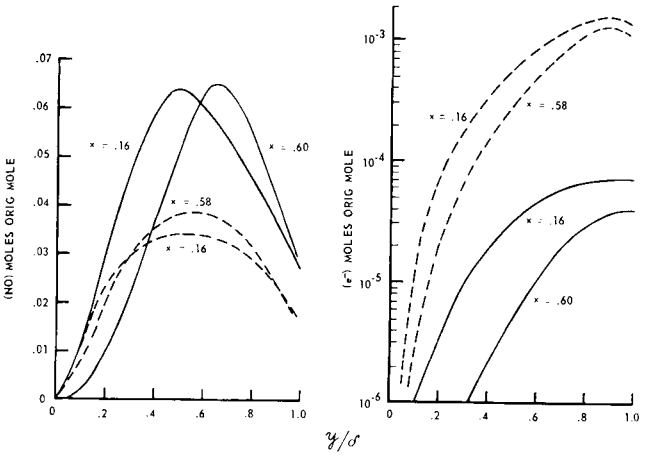

FIG. 12. Correlations of nitric oxide (NO) and electron (e^-) concentrations across nonequilibrium blunt-nose shock layer.

(4) Implications for Afterbody Flows

The preceding results have some obvious implications for the corresponding inviscid afterbody flows. The results indicate that for high-altitude conditions, oxygen and nitrogen atom mass concentrations tend to freeze in the nose region at levels below those corresponding to infinite-rate equilibrium behind the bow shock. For outer streamlines, in particular, this reduction from equilibrium dissociation can be large. It seems very likely that for these conditions the frozen atomic con-

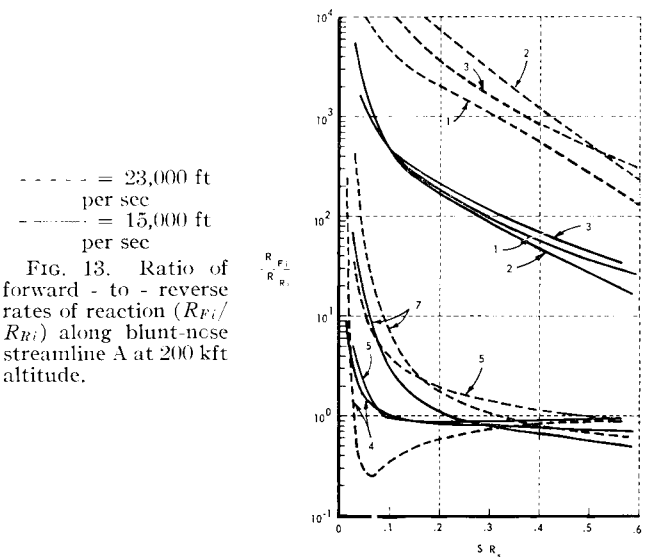

FIG. 13. Ratio of forward - to - reverse rates of reaction (R_{Fi}/R_{Ri}) along blunt-nose streamline A at 200 kft altitude.

TABLE 4.

Flight Velocity, U_∞, ft per sec	Altitude, z, ft $\times 10^3$	Shock Radius, R_s, ft	δ_0/R_s Present Noneq. Chemistry	δ_0/R_s Equilib. Chemistry	δ_0/R_s Frozen Chemistry	δ_0/R_s Ideal Gas
15,000	200	1.07	0.0676	0.0625	0.0890	0.113
23,000	200	0.0692	0.0666	0.0461	0.0805	0.108

centrations will prevail over an appreciable length in subsequent expansion of the flow over near-cylindrical afterbodies. This type of behavior is evidenced in the streamtube calculations of Ref. 15. In the flow expansion over the afterbody, the temperature and pressure are reduced, the latter dropping very strongly past the sonic point and following a blast-wave type of decrease downstream of the shoulder region. This behavior is very effective in quenching all chemical reactions.

The effects of nonequilibrium on the gasdynamics of the inviscid afterbody flow are determined by the concentrations of the atomic species. Therefore, for the type of conditions considered in the present examples it would appear that the inviscid afterbody flow could be computed in detail by usual ideal-gas characteristics methods with an effective (constant) specific-heat ratio determined from the atom mass concentrations frozen in the nose region. This type of approach has been taken previously by several authors.[15, 29] However, it has sometimes been assumed that the frozen atom concentrations are those appropriate to infinite-rate equilibrium immediately behind the shock or at the sonic line. As noted above, the present results indicate that this assumption, and therefore the dissociation enthalpy assumed to be frozen, can be considerably in error for the type of flow situations considered.

It may also be noted that the binary scaling of nonequilibrium blunt-nose flows at given velocity on the basis $\rho_\infty R_s$ = constant, as demonstrated by the present results, will automatically scale the corresponding inviscid afterbody flows correctly at a given Mach number if either the latter are frozen or else three-body recombination remains unimportant. Thus, any one numerical solution for the afterbody inviscid flow could be generalized or scaled in this way. Assuming the afterbody chemistry to be frozen, the blast-wave concept is readily modified to obtain an approximation to inviscid nonequilibrium effects on afterbody surface pressures, as previous authors have shown.[15, 29] The scaling of nonequilibrium blast-wave solutions on the above basis would appreciably extend their usefulness.

With respect to the simultaneous scaling of the viscous or boundary-layer flow over the afterbody, similar considerations apply here as for the nose region. If the afterbody boundary layer is chemically frozen—i.e., if atom diffusion dominates over recombination—as appears likely if the stagnation-point boundary layer as well as the outer inviscid flow is frozen, then the viscous afterbody flow is also scaled correctly by $\rho_\infty R_s$ = constant at given velocity and Mach number, provided the correct surface boundary conditions[12] are maintained.

(5) Concluding Remarks

This paper has discussed recent studies carried out at CAL of inviscid airflow over axisymmetric blunt bodies involving coupled chemical rate processes.

The results obtained with the reaction system considered illustrate the general importance of coupled chemical reactions at high enthalpy levels. For inviscid blunt-nose flow at flight conditions giving substantial nonequilibrium, exact solutions obtained by the inverse method illustrate nonequilibrium effects along streamlines which are common to plane normal shock flows. For example, the bimolecular exchange reactions play an important role in the kinetics of NO and N, and a characteristic maximum in NO concentration occurs. A basic difference from plane shock flow is the gasdynamic expansion occurring in the curved shock layer. This reduces post-shock reaction rates and contributes to the freezing of atom concentrations at levels substantially below those for infinite-rate equilibrium.

In the flight regime considered—i.e., where nonequilibrium prevails through the nose region—the chemical kinetics of the air are dominated by two-body collision processes. As a consequence, the entire inviscid airflow, including the coupled nonequilibrium phenomena, is amenable to binary scaling for given nose shape and flight velocity on the basis of a constant product of ambient density and body scale. This similitude, demonstrated with the exact solutions obtained by the inverse method, can also scale viscous and radiation phenomena occurring in the shock layer. The similitude provides a useful flexibility for hypersonic testing where it is applicable.

The results of the nose-flow study suggest that corresponding inviscid afterbody flows at high altitudes may exhibit the reduced atom concentrations effectively frozen in the nose region. In this case, analysis of the afterbody flow may be considerably simplified by the use of frozen-flow characteristics methods and by application of binary scaling.

References

[1] Freeman, N. C., *Dynamics of a Dissociating Gas; III. Non-Equilibrium Theory*, J. Fluid Mech., Vol. 4, Pt. 4, 1958.

[2] Lick, W., *Inviscid Flow Around a Blunt Body of a Reacting Mixture of Gases*, Rensselaer Poly. Inst., TR AE 5810, May 1958, and TR AE 5814, Dec. 1958.

[3] Li, T. Y., *Recent Advances in Nonequilibrium Dissociating Gasdynamics*, ARS Jour., Feb. 1961.

[4] Duff, R. E., and Davidson, N., *Calculation of Reaction Profiles Behind Steady State Shock Waves; II. The Dissociation of Air*, J. Chem. Phys., Vol. 31, No. 4, Oct. 1959.

[5] Lin, S. C., and Teare, J. D., Bull. Am. Phys. Soc., Ser. II, Vol. 4, p. 195, 1959.

[6] Wray, K. L., "Chemical Kinetics of High Temperature Air," *Hypersonic Flow Research, Vol. 7—Progress in Astronautics and Rocketry*, pp. 181–204; Academic Press, New York, 1962.

[7] Hall, J. G., and Russo, A. L., "Studies of Chemical Nonequilibrium in Hypersonic Nozzle Flows," *Proc. 1st Conference on Kinetics, Equilibria, and Performance of High Temperature Systems*, Butterworths, London, 1960; also, CAL Rep. AD-1118-A-6, Nov. 1959.

[8] Wurster, W. H., and Marrone, P. V., *Study of Infrared Emission in Heated Air*, CAL Rep. QM-1373-A-2, May 1960, and QM-1373-A-4, June 1961.

[9] Eschenroeder, A. Q., Boyer, D. W., and Hall, J. G., *Nonequilibrium Expansions of Air With Coupled Chemical Reactions*, Phys. Fluids, Vol. 5, No. 5, May 1962; also, CAL Rep. AF-1413-A-1, May 1961.

[10] Hall, J. G., Eschenroeder, A. Q., and Marrone, P. V., *Inviscid Hypersonic Airflows With Coupled Nonequilibrium Processes*, IAS Paper No. 62-67, 30th Annual IAS Meeting, Jan. 22–24, 1962; also, CAL Rep. AF-1413-A-2, AFOSR 2072, May 1962.

[11] Eschenroeder, A. Q., *Ionization Nonequilibrium in Expanding Flows*, ARS Jour., Vol. 32, No. 2, Feb. 1962.

[12] Gibson, W. E., *Dissociation Scaling for Nonequilibrium Blunt-Nose Flows*, ARS Jour., Vol. 32, No. 2, Feb. 1962.

[13] Eschenroeder, A. Q., Daiber, J. W., Golian, T. C., and Hertzberg, A., *Shock Tunnel Studies of High-Enthalpy Ionized Airflows*, paper presented at AGARD Conf. on High Temperature Aspects of Hypersonic Flow, April 3–6, 1962.

[14] Vincenti, W. G., *Calculations of the One-Dimensional Nonequilibrium Flow of Air Through a Hypersonic Nozzle—Interim Report*, Stanford Univ., Dept. Aero. Eng., Rep. 101, Jan. 1961.

[15] Vaglio-Laurin, R., and Bloom, M. H., "Chemical Effects in External Hypersonic Flows," *Hypersonic Flow Research, Vol. 7—Progress in Astronautics and Rocketry*, pp. 205–254; Academic Press, New York, 1962.

[16] Lin, S. C., and Teare, J. D., *A Streamtube Approximation for Calculations of Reaction Rates in the Inviscid Flow Field of Hypersonic Objects*, AVCO Res. Note 223, Aug. 1961; also, Proc. 1961 AF/Aero. Corp. Symp. on Ballistic Missile and Aerospace Technology.

[17] Hammerling, P., Teare, J. D., and Kivel, B., *Theory of Radiation From Luminous Shock Waves in Nitrogen*, Phys. Fluids, Vol. 2, pp. 422–426, 1959.

[18] Treanor, C. E., and Marrone, P. V., *The Effect of Dissociation on the Rate of Vibrational Relaxation*, CAL Rep. QM-1626-A-4, Feb. 1962.

[19] Penner, S. S., *Introduction to the Study of Chemical Reactions in Flow Systems*, Butterworths, London, 1955.

[20] Gibson, W. E., and Marrone, P. V., *A Similitude for Nonequilibrium Phenomena in Hypersonic Flight*, Paper presented at AGARD Conf. on High Temperature Aspects of Hypersonic Flow, April 3–6, 1962.

[21] Gibson, W. E., and Marrone, P. V., *A Correspondence Between Nonequilibrium Normal Shock and Blunt-Body Flows* (to be published).

[22] Camm, J., Kivel, B., Taylor, R., and Teare, J. D., *Absolute Intensity of Non-Equilibrium Radiation in Air and Stagnation Heating at High Altitudes*, J. Quantitative Spec. and Radiative Transfer, Sep. 1961; also, AVCO Res. Rep. 93, Dec. 1959.

[23] Hertzberg, A., Wittliff, C. E., and Hall, J. G., "Development of the Shock Tunnel and Its Application to Hypersonic Flight," *Hypersonic Flow Research, Vol. 7—Progress in Astronautics and Rocketry*, pp. 701–758; Academic Press, New York, 1962.

[24] Hayes, W. D., and Probstein, R. F., *Hypersonic Flow Theory*, Academic Press, New York and London, 1959.

[25] Teare, J. D., Hammerling, P., and Kivel, B., *Theory of the Shock Front; II. High Temperature Reaction Rates*, AVCO Res. Note 133, June 1959.

[26] Scala, S. M., *Hypersonic Viscous Shock Layer*, ARS Jour., Vol. 29, pp. 520–521, July 1959.

[27] Maslen, S. H., and Moeckel, W. E., *Inviscid Hypersonic Flow Past Blunt Bodies*, Journal of the Aeronautical Sciences, Vol. 24, No. 9, Sep. 1957.

[28] Li, T. Y., and Geiger, R. E., *Stagnation Point of a Blunt Body in Hypersonic Flow*, Journal of the Aeronautical Sciences, Vol. 24, No. 1, Jan. 1957.

[29] Whalen, R. J., *Viscous and Inviscid Nonequilibrium Gas Flows*, IAS Paper No. 61-23, IAS 29th Annual Meeting, New York, Jan. 23–25, 1961.

[30] Byron, S. B., *Interferometric Measurement of the Rate of Dissociation of Oxygen Heated by Strong Shock Waves*, Cornell Univ. Rep., 1958; J. Chem. Phys., Vol. 30, pp. 1380–1392, 1959.

[31] Wray, K. L., Teare, J. D., Kivel, B., and Hammerling, P., *Relaxation Processes and Reaction Rates Behind Shock Fronts in Air and Component Gases*, AVCO Res. Rep. 83, Dec. 1959.

[32] Glick, H. S., Klein, J. J., and Squire, W. J., *Single-Pulse Shock Tube Studies of the Kinetics of the Reaction* $N_2 + O_2 \rightleftarrows 2\ NO$ *Between 2000–3000°K*, J. Chem. Phys., Vol. 27, p. 850, 1957.

[33] Lin, S. C., Fyfe, W. I., and Neal, R. A., *Rate of Ionization Behind Shock Waves in Air*, AVCO Res. Rep. 105, Sep. 1960.